Advances in Science and Technology Research Journal

*Advances in Science and Technology Research Journal*, 2026, 20(10), 87–104
https://doi.org/10.12913/22998624/224333
ISSN 2299-8624, License CC-BY 4.0

Received: 2026.05.11
Accepted: 2026.07.09
Published: 2026.09.01

# Identification of forging die wear mechanisms in the hot forging process

Grzegorz Ficak[1,2], Aneta Łukaszek-Sołek[1], Łukasz Lisiecki[1], Tomasz Śleboda[1*], Piotr Bathelt[2]

[1] Faculty of Metals Engineering and Industrial Computer Science, AGH University of Krakow, al. Mickiewicza 30, 30-059 Krakow, Poland
[2] GK FORGE, ul. Przemysłowa 10, 43-440 Goleszów, Poland
* Corresponding author's email: sleboda@agh.edu.pl

## ABSTRACT

This study presents an analysis of degradation mechanisms of a forging die used in the hot forging process of a counterweight forgings. The investigated tool was made of hot-work X37CrMoV5-1 (1.2343) tool steel. The study was aimed at identification of the dominant degradation mechanisms of a hot forging die insert made of 1.2343 steel used under industrial conditions and correlation of those mechanisms with the microstructure, hardness distribution and operational thermal loading. The research methodology included macroscopic and microscopic examinations of the die working surface, microstructural analysis using optical microscopy and scanning electron microscopy (SEM), fracture surface investigations, hardness measurements across the tool cross-section, numerical analysis of the die forging process, and dimensional assessment using 3D scanning. The results showed that the dominant degradation mechanisms were connected with thermal fatigue, abrasive wear, adhesive wear, and crack propagation in the subsurface layer of the die. Microstructural observations revealed a tempered martensitic structure as well as local microstructural banding promoting stress concentration and crack initiation. SEM analysis confirmed the brittle character of cracking with the presence of intergranular fracture zones. Hardness measurements indicated a non-uniform hardness distribution within the tool and an increased hardness of the surface layer exceeding 57 HRC. The obtained results indicate that the degradation of the forging die resulted from the combined effects of high temperature, mechanical loads, and intensive friction occurring during tool operation. The identified degradation mechanisms provide important information for improving the durability and operational reliability of forging tools used in hot forging processes.

**Keywords:** forging, tool wear, steel, microstructure, wear mechanisms.

## INTRODUCTION

The durability of tools used in hot forging processes is a key parameter that determines manufacturing efficiency, the consistent quality of forgings, and the total operating costs of the production system. The coexistence of numerous, interrelated degradation mechanisms means that the description of wear phenomena in forging dies requires a multiscale approach, i.e., ranging from local tribological and thermal conditions to the global characteristics of the tool's thermomechanical loads [1, 2]. The wear mechanisms in hot forging are complex and synergistic in nature, whereas their relative contribution depends on the local tribological, thermal, and stress conditions in the tool-workpiece contact zone [3, 4]. Under industrial conditions, the predominant forms of wear are abrasive, adhesive, and oxidative wear, thermomechanical fatigue (TMF), classical mechanical fatigue, and cracking initiated in stress concentration zones or in the presence of post-processing defects [5–7]. In industrial service these mechanisms do not occur in isolation but overlap during successive forging cycles, generating a complex, evolving state of damage in the tool's surface layer [8, 9]. High temperatures and cyclic loads lead to a reduction in surface hardness, accelerating the process of wear and plastic deformation. In contrast, in the areas exposed to large temperature gradients and frequent contact with the cooling-lubricating fluid, thermal-mechanical fatigue predominates. In the areas of intense flow of the charge material (narrowing, narrow ribs, protrusions, radius zones), abrasive and adhesive wear predominate, accelerated by local thermal softening (high temperatures and repeated cycles reduce hardness accelerating wear and deformation), while in the areas with sharp geometric transitions and varying cross-sections, fatigue damage and brittle fracture accumulate [9, 10]. A clear correlation has been established between the quality of tool pre-machining (grinding, milling, finishing) and their service life [11, 12]. Studies by Dalbosco [13] and Killmann [14] on forging tools confirm that initial compressive stresses and properly designed geometry, taking into account radius zones, are an effective way to reduce the amplitude of tensile stresses and extend tool life, which can largely be applied to hot forging conditions as well. Design guidelines that take into account tool radii, prestressing, and improvements in the homogeneity of the feedstock can reduce stress concentrations and improve fatigue performance. Of particular significance are the results of studies conducted by Pereira [15] and Lee [16], which indicate that minimizing sharp transitions and precisely controlling of edge radii limit local stress concentrations, reducing both wear intensity and the risk of fatigue crack initiation in critical metal flow areas. Modifying the die geometry, controlling forging parameters, and applying integrated advanced heat transfer models reduce stresses in the tool and improve its durability [17]. Previous studies on hot forging tools have often focused primarily on the dies made of chromium-molybdenum-vanadium steel, new-generation steels produced by powder metallurgy, and alloys with modified chemical compositions. The conducted research is typically based on three complementary pillars: laboratory tests (thermomechanical fatigue, tribological testing, nano- and microindentation, hardness measurements, and residual stress distributions), advanced FEM simulations coupling temperature and stress distributions with wear models, and verification under real industrial process conditions, which enables both calibration and validation of the developed tool life models [18, 19]. Moreover, modifications to the chemical composition (additions of Nb, W, V, Cr) as well as new generations of steels produced by powder metallurgy, including nanostructured materials and alloys with enhanced thermal stability, which enable the achievement of a favorable combination of high strength, creep resistance, and adequate ductility within typical forging temperature ranges, are being developed [20, 21]. The introduction of advanced PM (powder metallurgy) steels [22, 23], as well as composite materials and bimetallic solutions, has made it possible to significantly reduce thermal softening and cracking, as confirmed by the studies performed under industrial conditions. The works of Li [24] and Duchek [25] described steels with enhanced thermal stability and resistance to softening, achieved through a controlled nanostructure and the selection of alloying elements such as Nb. Studies on Cr-Mo-V steels, steels with Nb and W additions, and steels reinforced by oxide dispersion (ODS) [24, 26] have shown that increasing the Nb content by 0.2–0.5 wt.% improves hot strength and fatigue resistance. The Nb(C, N) inclusions formed during heat treatment act as barriers to dislocation motion at high temperatures. Multi-criteria decision-making methods based on fuzzy logic are also being developed to identify optimal tool steels for various forging conditions (e.g., 2999 EFS SUPRA for press forging, 1.2714 for hammer forging) [27]. It has been demonstrated that the chemical composition and rheology of lubricants [28, 29] (oil- and water-based graphite lubricants, graphite-free systems, borate-based agents), their application method [18] (spraying, oil mist, solid coatings), and dosing parameters significantly influence the coefficient of friction, the intensity of heat transfer in the tool-workpiece contact zone, as well as the formation of transition layers on the die surface, which directly affect the local wear rate and the development of thermal cracks. Under the conditions of insufficient cooling and lubrication, abrasive wear remains the dominant mechanism of degradation, whereas in modern systems with intensive lubrication and precise temperature control, the main factor limiting tool life is thermal-mechanical fatigue, leading to the formation of a network of surface microcracks (heat-checking) and the gradual degradation of the surface layer's integrity. Improperly selected lubrication conditions result in increased friction, localized overheating, and intensified abrasive wear, whereas optimally selected lubricants can simultaneously act as a thermal barrier and a separating layer, prolonging the incubation time of fatigue cracks. Additionally, controlled preheating of the tool and workpiece, along with integrated cooling and spray control systems, reduce temperature gradients and thus the amplitude of cyclic thermal stresses [30, 31]. The studies by Jeong [28], Lee [29], and Hawryluk [2, 18] demonstrated that the proper selection of graphite lubricants (oil-based and water-based) and the optimization of their application method (dose, frequency, spray parameters, and geometry) allow for a significant reduction in the coefficient of friction, the thermal load on the die, and the rate of its wear. An integral part of the modern research approach is the use of advanced computational tools based on the finite element method [32–38]. A trend toward an integrated approach, combining FEM simulations, experimental validation, and in situ measurements under industrial conditions, is becoming increasingly evident [33, 39]. Dudkiewicz [40] presented examples of low-waste precision forging technologies in which modifications to tool geometry, forging process parameters, and the cooling system - based on numerical analysis - lead to reduced wear, lower energy consumption, and improved dimensional accuracy of forgings. The significant contributions of Kim [41] and Virtanen [42] regarding the quantitative description of the softening of tool steels using the tempering parameter made it possible to correlate the temperature history of the forging cycle with changes in hardness and resistance to plastic deformation. Concurrently, Schlayer [43] proposed a viscoplastic material model for X38CrMoV5-3 steel, taking into account microstructural evolution (dislocation density, carbide coagulation and dissolution) and the thermal fatigue effect, which allowed for the reproduction of cyclic plastic deformation and progressive softening under thermomechanical loads characteristic of die forging. Integrated numerical-experimental analyses [44, 45], in which the data from fatigue tests of tool steels under thermomechanical forming conditions are coupled with simulation results, are used to verify the models based on 3D wear measurements of actual dies and microscopic diagnostics of the failure surface. Monitoring the cyclic thermal history of the tool through the integration of temperature sensors in the dies makes it possible to simultaneously reduce softening and surface layer degradation while improving the dimensional and geometric accuracy of a product [30]. Many publications employ virtual variation of die geometries (radii, chamfers, die cavity depths) and process conditions (forging temperature, strain rate, lubrication strategy), which enables preliminary optimization of the process setup without the need for costly industrial trials [36, 37].

Despite this extensive research, most studies analyze individual degradation mechanisms, specific surface treatments or particular classes of tool steels, often under laboratory conditions or with simplified service histories. There is still a lack of comprehensive, multiscale studies that correlate the microstructure, hardness distribution and service-induced thermal loading for dies withdrawn from real industrial hot forging operations. In particular, systematic analyses of hot forging dies made of steel 1.2343 that exhibit local chemical composition anomalies are scarce, although such anomalies may significantly affect microstructural stability, softening behavior and crack susceptibility under cyclic thermal–mechanical loads.

The scientific novelty of the present study lies in the identification and quantitative characterization of dominant degradation mechanisms of an industrially operated 1.2343 die insert. The study combined 3D scanning of the worn die cavity with optical microscopy (OM), scanning electron microscopy (SEM), numerical modeling (FEM), hardness mapping, and Charpy impact tests in order to identify the dominant degradation mechanisms and relate them quantitatively to the local microstructure and property gradients. By correlating the measured hardness distribution and microstructural changes with estimates of the thermal loading during service, the work aimed to bridge the identified research gap and provide a more complete description of the degradation of hot forging dies under real industrial conditions for steel 1.2343.

## EXPERIMENTAL

The forging process was carried out on a screw press with a nominal pressure of 400 tons and a double ejector. Prior to production, the tools were heated using a gas burner to a surface temperature of approximately 220–250 °C. The die-forged blank was made of S355J2 steel in the as-rolled condition. The billet temperature, measured by a pyrometer mounted on the heater, ranged from 1150 to 1200 °C. When the operator removed the billet from the chute, the forging temperature was 1100 to 1150°C. The temperature of the tools during the forging process was also measured using a Benetech GM1651 pyrometer. A QH PRESSMAX™ FWG 1402 lubricant in the form of a suspension of graphite in water (1:10) was used during the forging process. After each cycle, the lubricant was applied evenly to the tool surfaces using special nozzles. At the same time, the die cavities were blown with compressed air to remove the remaining scale. The forging die insert was examined. The component was a finish-forging die that failed prematurely by cracking. It was mounted in a specially designed housing. The tool was rendered unusable after producing approximately 700 forgings. It was made of X37CrMoV5-1 (1.2343) tool steel. This tool steel is a combination of various chemical elements, specially designed for use at high temperatures. This steel is also commonly used for pressure molds, dies and forging inserts, extrusion tools, and press components. Table 1 presents the chemical composition of 1.2343 tool steel in accordance with the EN ISO 4957:2018 standard, along with average values obtained from experimental measurements. The chemical analysis was performed using a Foundry-Master UV optical emission spectrometer (OES), which enabled rapid and precise determination of the alloying elements.

The 3D scanning of the investigated die was performed using an eviXscan 3D Heavy Duty Quadro scanner. To accurately measure dimensional deviations of the die after industrial service and to identify the areas with the highest degree of degradation, 3D scanning technology was employed, enabling detailed analysis of the tool surface in terms of dimensional and geometric changes. The obtained data were imported into Geomagic Control X software, where the scan registration against with the CAD reference model was carried out using a best-fit alignment algorithm with six degrees of freedom of spatial transformation. Flat, unworn base surfaces of the tool were used as reference areas for the initial alignment. According to the manufacturer's specification, the scanner's metrological accuracy was ±0.02 mm and the scanning resolution was 0.05 mm. The aligned scan enabled visualization of the wear distribution on the die surface and identification of the most degraded regions. It should be noted that no additional validation of the measurement procedure, such as repeated scanning or reference measurements with a coordinate measuring machine, was performed.

The insert die was then cut into smaller pieces, from which samples were made for mechanical property and microstructure testing of the tool. In order to obtain the microstructure, the test samples were etched with a 6% nital solution for approximately 30 seconds. Following the etching process, microstructural studies were conducted on a light microscope. The microstructure of the tool material from which the forging tool was made was analyzed in the first instance in the microstructural study. The investigation also encompassed the analysis of the cracks formation. The microstructure of the subsurface layer was examined using an MMT 120BT optical microscope with an HDCE-X3 camera and a ThermoFisher Phenom XL scanning electron microscope. Hardness measurements were made with a Struers Duramin 40 M1 hardness tester. For each investigated region, at least three independent hardness measurements were performed, and the reported values represent average values.

The die insert was then subjected to a series of tests in order to ascertain its properties and microstructure. Figure 1 illustrates the tool alongside the designated areas to be tested. The chemical composition of the steel was analyzed in area 1 shown in Figure 1. Impact tests in two directions were conducted on the samples taken from areas 5 and 6. Hardness measurements were performed on samples taken from the areas 2 and 3 (see Figure 1). Fracture breakthrough was examined in

**Table 1.** The chemical composition (wt. %) of the investigated tool material (avg. measured) in relation to the EN ISO 4957: 2018 standard

| Parameter | C | Si | Mn | P | S | Cr | Mo | V |
|---|---|---|---|---|---|---|---|---|
| Min. (standard) | 0.33 | 0.8 | 0.25 | - | - | 4.8 | 1.1 | 0.3 |
| Max (standard) | 0.41 | 1.2 | 0.50 | 0.03 | 0.02 | 5.5 | 1.5 | 0.5 |
| Avg. (measured) | 0.35 | 1.07 | 0.36 | 0.042 | 0.02 | 4.8 | 1.1 | 0.3 |

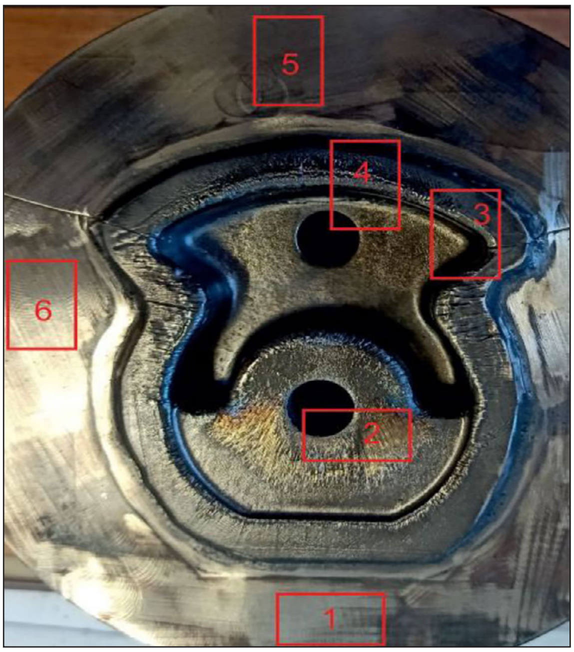


**Figure 1.** Investigated tool with marked areas used for testing

area 4. All of these procedures were carried out using a scanning electron microscope.

A numerical analysis of the die forging process was performed using the QForm UK software to identify the failure mechanism of the die insert. The following boundary conditions were adopted for the numerical calculations: charge temperature of 1150 °C, tool temperature of 250 °C, a graphite-in-water solution was applied as a lubricant, friction coefficient of 0.4. The remaining boundary conditions were also adopted in accordance with the forging test conditions. The analysis examined the distribution of equivalent stress, maximum principal stress $\sigma_1$, mean stress, elastic strain, and temperature in the tool's working area. The simulation results were compared with the actual industrial damage to the die after use. Particular attention was paid to the correlation between stress concentration zones and the location of crack initiation and propagation. The simulation covered all three operations of the hot forging sequence. The coupled deformation task mode was applied, in which the elasto-plastic stress and strain state of the tool is resolved simultaneously with workpiece deformation at selected simulation steps. Heat transfer was modeled in the coupled mode, with the temperature field calculated throughout the full tool volume and accounting for heat exchange with the workpiece, the environment, and the contacting tools. The purpose of the analysis was not intended as a quantitative prediction of die service life, but to identify the critical stress concentration regions and correlate them with the observed locations of damage.

## RESULTS AND DISCUSSION

### Identification of damage and wear level of tools after service

The examination of the tools withdrawn from service after producing a batch of 700 forgings began with an assessment of their wear. In the first stage, three-dimensional scanning of the die working surface was carried out using a 3D scanner, which enabled precise reconstruction of the tool geometry and evaluation of dimensional deviations relative to the reference CAD model. Figure 2 presents the post-exploitation scan of the forging die. Three-dimensional scanning performed after tool use showed acceptable geometric deformations, indicating dimensional stability within allowable workshop tolerances and adequate precision of the forming process. However, macroscopic analysis revealed the presence of cracks in the die cavity bottom area as well as signs of abrasive wear in the so-called "spider web" region, pointing to local mechanical and thermal overloads and unfavorable frictional conditions.

The analysis of the results showed that the dimensional changes were minimal and remained within acceptable workshop tolerances, indicating that the forming accuracy was largely preserved across most areas of the tool (Figure 3). The 3D scan analysis indicated that the largest dimensional deviations were localized in the most highly loaded regions of the die cavity. Localized material

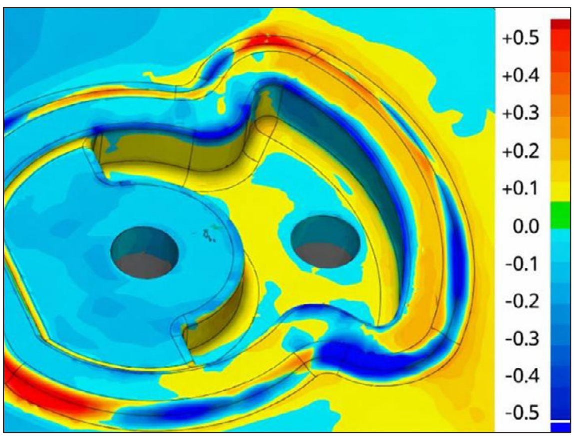


**Figure 2.** Post-exploitation scan of the forging die

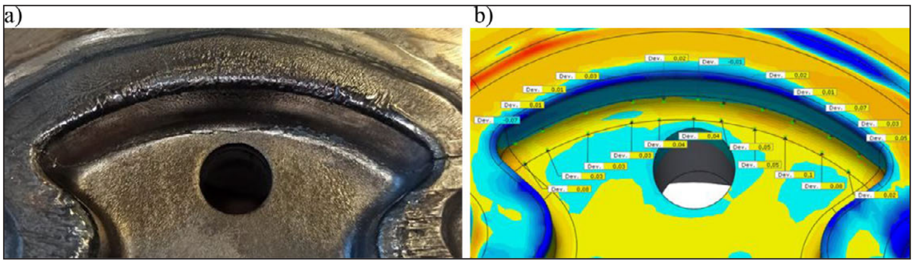


**Figure 3.** Bottom die: a) Decommissioned, b) Dimensional deviations relative to the reference model in the area of die damage

loss and surface degradation were particularly pronounced in the "spider web" region and near the bottom of the die cavity, where cracks and abrasive wear marks were mechanisms were subsequently identified by macroscopic examination. The macroscopic analysis revealed the presence of cracks in the rounded bottom region of the die cavity. Their occurrence indicates localized material overloading, most likely resulting from the accumulation of thermal and mechanical stresses occurring during tool operation. In the remaining regions of the tool, no significant signs of degradation were observed, except in the web area, where distinct traces of abrasive wear were identified. This type of damage indicates intensive contact between the workpiece and the tool surface, as well as unfavorable friction conditions in this zone.

## Detailed microstructural analysis of the examined steel

A detailed microscopic analysis of the examined material (Figure 4) indicates that the microstructure of the investigated tool steel is characterized by the presence of tempered martensite, which is typical for the materials subjected to heat treatment processes. Throughout the entire cross-section, a fine needle-like or fine plate-like structure of tempered martensite forming a dense and relatively homogeneous grain network is visible. This martensite is a very hard and wear-resistant structure formed during rapid cooling, while the tempering process improves ductility and reduces internal stresses.

The microscopic images show characteristic martensitic laths forming a dense and regular network within the steel microstructure. Alternating zones with slightly different densities of martensitic laths and carbide concentrations can also be observed. Based on the comprehensive analysis, it can be concluded that the base material exhibits high homogeneity and lacks visible defects such as cracks, inclusions of critical size, or metallurgical imperfections.

Figure 5 shows a microscopic image of sample 3 (sample taken from area 3 shown in Figure 1), obtained using an optical microscope at 2.5× magnification. A distinct microstructural banding is observed, likely resulting from the rolling process of the ingots. This banding represents a material defect characterized by microstructural heterogeneity, which may adversely affect the mechanical properties of the investigated steel. Within the bands, non-metallic inclusions and areas of incomplete grain recrystallization may be present, resulting from incomplete structural restoration during hot deformation. Such a microstructure can lead to localized stress concentrations and reduced fatigue resistance of the material. The observed banding may also promote local microstructural anisotropy, potentially influencing crack propagation paths under thermo-mechanical loading conditions.

The microstructure in the immediate vicinity of the working surface of the die differs from the structure in the deeper layers. This is a result of the intense heat influence from the billet on the tool surface. After the forging process, the die is subjected to lubrication and cooling, which leads to partial hardening and microstructural changes in the layers near the tool working surface. As the distance from the working surface increases, the material is still heated which influences the resulting microstructure (Figure 6).

Figure 7 shows a crack located in the samples taken from areas 3 and 4 (shown in Figure 1), formed as a result of thermal fatigue. The damage mechanism is a consequence of the high temperature of the billet material and the stresses generated during the die cavity filling process. Crack initiation and propagation occurred along the directions of the highest stresses.

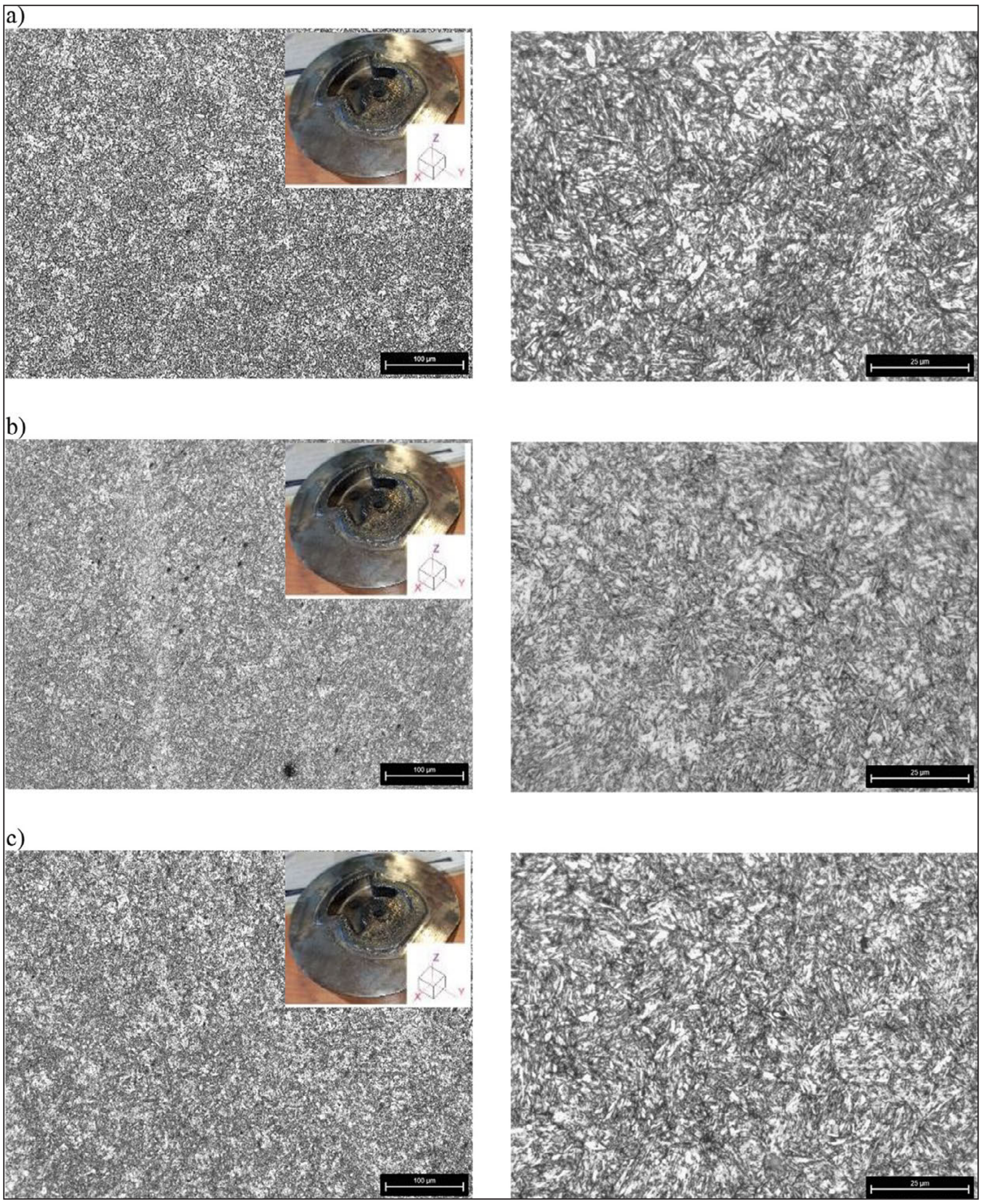


**Figure 4.** Microstructure of the examined tool steel: a) in the XY plane, b) in the XZ plane, c) in the YZ plane shown in Figure 1

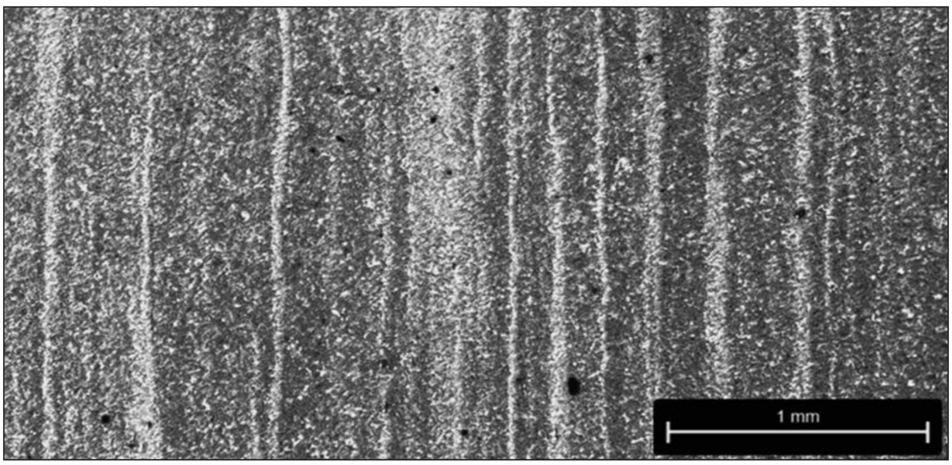


**Figure 5.** Banded microstructure of the examined steel (sample taken from area 3 shown in Figure 1)

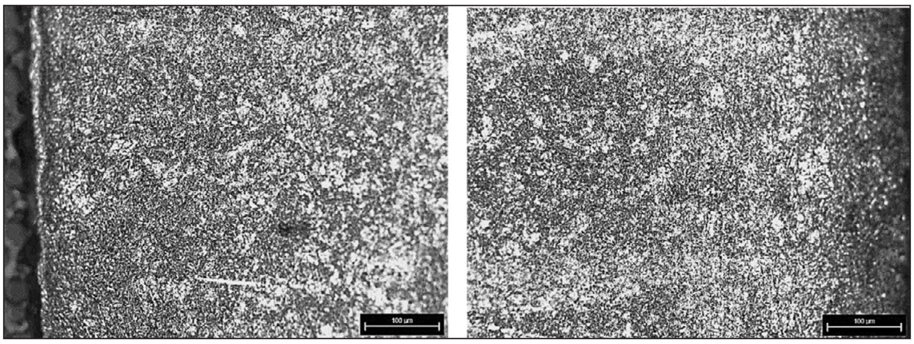

**Figure 6.** Microstructural region near the working surface of the die – (sample taken from area 2 shown in Figure 1)

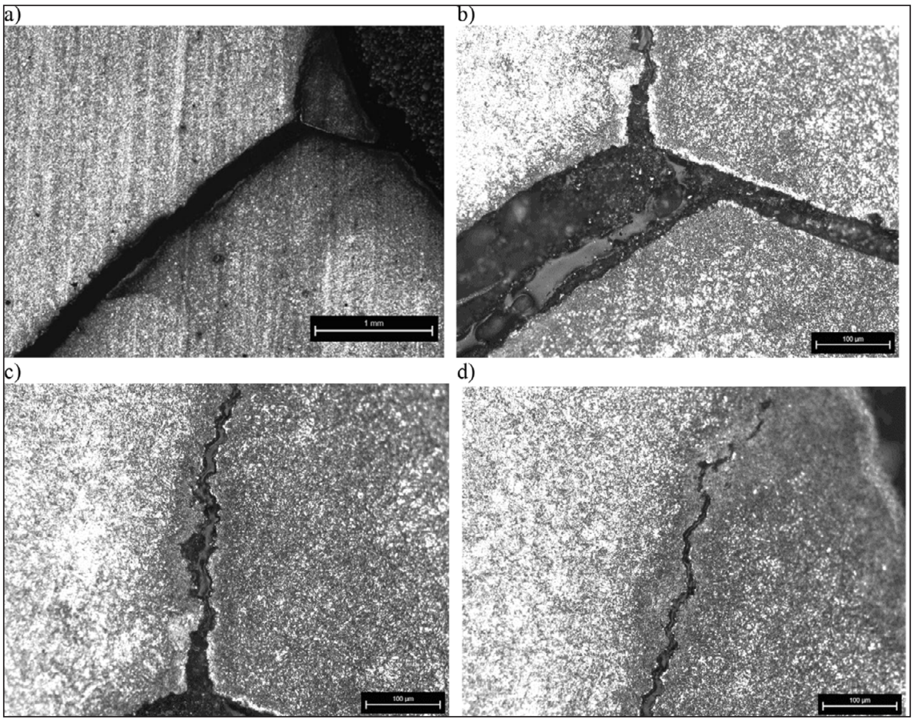


**Figure 7.** Crack developing in the tempered martensitic microstructure of hot work tool steel (samples taken from area 3 and 4 shown in Figure 1): a) general view; b) advanced microstructural degradation; c, d) crack propagation into the material

In the immediate vicinity of the crack, a fine needle-like structure of tempered martensite with numerous bright carbide precipitates located at the boundaries of subgrains and prior austenite grains can be observed. The crack intersects both martensitic needles and carbide bands, locally branching and forming a network of smaller microcracks, which indicates propagation under thermo-mechanical fatigue conditions.

Along the edges of the crack, darkened zones and small material losses are visible, interpreted as the result of oxidation of the crack surface and erosion occurring during further tool operation. The crack develops in a direction perpendicular to the highest tensile stresses, which in forging dies appear mainly in the subsurface layer, particularly in the areas of the highest temperature gradient and direct contact with the forging.

The crack propagates along the boundaries of martensite packets and the regions with locally modified microstructure. Secondary microcracks branching from the main crack are also visible, indicating the accumulation of thermo-mechanical stresses and progressive weakening of the structural cohesion of the material.

This type of microstructural image is characteristic of fatigue cracking in hot forging tools, where the crack initiates at the working surface and then propagates into the interior of the material as the number of forging cycles increases. The observed crack can be primarily associated with the thermal fatigue mechanism, which is one of the dominant forms of degradation in hot forging dies.

Cyclic heating and cooling lead to the formation of thermal stresses that initiate microcracks on the working surface of the tool. In subsequent cycles, these cracks propagate deeper into the material, eventually leading to macroscopic damage of the die.

The fracture surface analysis performed using scanning electron microscopy (SEM) indicates a brittle fracture character with distinct intergranular fracture zones, resulting from prolonged mechanical loading at elevated temperature and confirming the significant influence of thermal processes on material degradation.

During a detailed microstructural analysis of the tool, additional cracks were identified in the region of the forging die draft angle (area 4), as documented in Figure 8. These cracks, similar to the previously described damage, resulted from thermal fatigue caused by cyclic temperature changes and thermomechanical stresses generated during the hot die forging process. The combined effect of high temperatures and intense frictional forces led to directional propagation of cracks along the microstructural banding of steel, which is a characteristic failure mechanism in the materials with strong structural anisotropy. Microscopic observations indicate that the cracks developed following the orientation of the microstructural bands until neighbouring cracks coalesced, significantly increasing local stress concentrations and promoting further mechanical defects. This condition substantially reduces the load-bearing capacity and resistance to operational stresses of a material, leading to localized spalling of tool fragments. Continued use at this stage would result in rapid deterioration of mechanical properties and could cause premature tool failure. This highlights the importance of timely monitoring and replacement of damaged components to prevent severe technical and economic consequences.

Figure 9 presents an image obtained using optical microscopy, showing a section of the lower die in the region of the flash groove transition. In this area, a pronounced banded microstructure can be observed, resulting from the rolling process of the billet, as well as a thermally affected zone located directly adjacent to the die's working surface - an effect of repeated exposure to high temperatures from the workpiece combined with intensive cooling and lubrication of the tool. Within the examined region, the initiation and propagation of cracks were also identified. These cracks are located both on the forging draft angle and along the radius of the transition edge leading into the flash groove. They are characteristic of the damage caused by thermo-mechanical fatigue. Importantly, a thin layer of material appears to have been displaced from the rounded transition radius - this layer was likely mechanically "sheared off" and transported toward the flash pocket during the die-filling process. This phenomenon indicates a significant local influence of friction forces and temperature, leading to intense material wear in the transitional zone. The displaced material was subsequently compacted by the advancing billet, further contributing to the formation of surface discontinuities and local defects that could potentially act as initiation sites for additional tool damage in subsequent forging cycles.

As part of further investigations, fracture surface analysis was conducted on sample 4 (sample taken from area 4 shown in Figure 1) using scanning electron microscopy (Figure 10). The initial stage of the study focused on the working surface

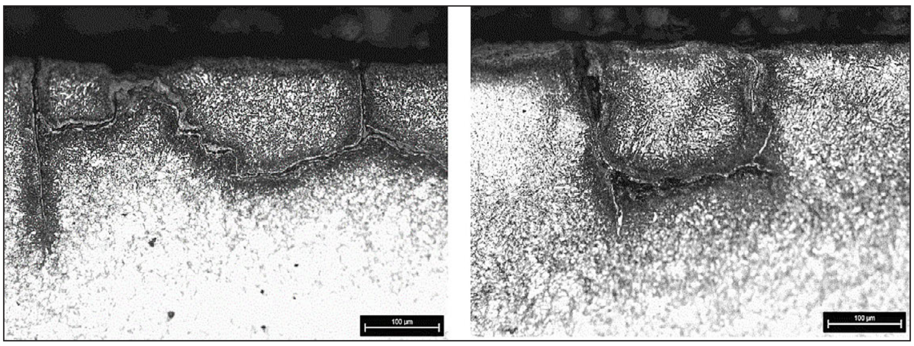

**Figure 8.** Cracks formed on the forge draft angle – area 4 shown in Figure 1

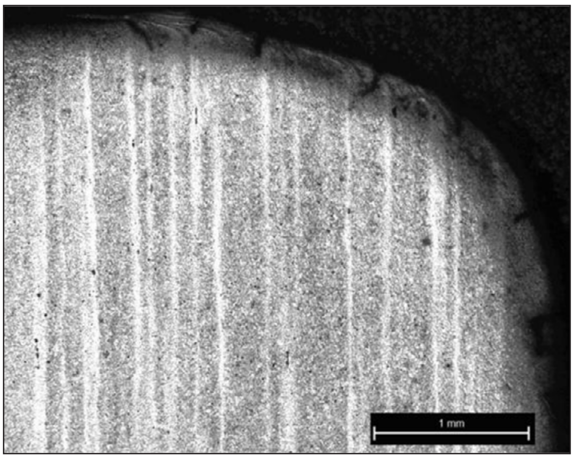


**Figure 9.** Rounded edge at the transition to the web

of the forging die, which during operation is exposed to high temperature, mechanical pressure, and direct contact with the deformed material.

SEM observations indicated that thermal fatigue was the dominant wear mechanism responsible for crack initiation and propagation. The crack propagated along the boundaries of martensite packets, indicating local stress concentration and weakening of the microstructural cohesion. In the immediate vicinity of the crack, secondary microcracks and zones of intensive thermo-mechanical deformation were observed. This microstructural image clearly indicates that the crack has an operational rather than technological

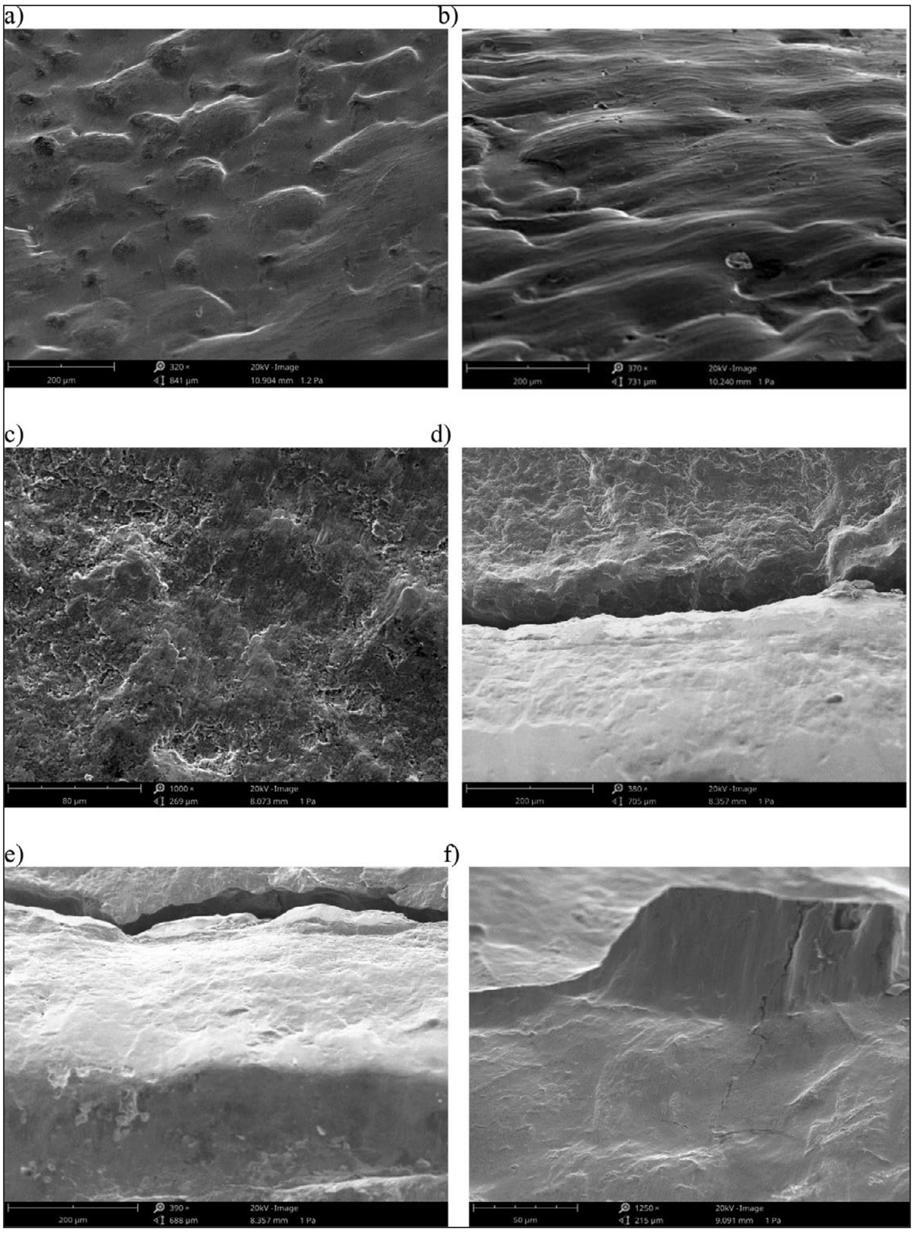


**Figure 10.** Working surface of the die – area 4 shown in Figure 1: a) central region; b) fillet radius; c) crack initiation site; d, e) crack morphology; f) crack propagation into the material

origin, developing gradually during tool service. The degradation process was additionally intensified by adhesive wear, abrasive wear, and local microstructural degradation caused by long-term exposure to elevated temperature. Numerous oxidation products (oxides, scale) were also visible on the surface, confirming prolonged exposure to high temperatures and repeated heating–cooling cycles of the tool surface. The cracks were identified as surface cracks, oriented perpendicular or at a small angle to the working surface, which is typical for thermal fatigue phenomena known as heat checking.

The examined area of the tool also revealed characteristic surface peaks and cavities, indicating non-uniform wear of the material. This phenomenon is directly related to the presence of microstructural banding, previously identified in the analyzed die. The bands were oriented perpendicular to the working surface, leading to local differences in mechanical properties. The regions corresponding to the cavities exhibited lower hardness and greater susceptibility to abrasive wear as compared with more homogeneous regions. Such uneven wear of the working surface may reduce forming precision and accelerate tool degradation, making microstructural banding an important factor in the assessment of wear mechanisms in forging tools. Cyclic heating of the die during contact with the hot forging and its subsequent rapid cooling led to the formation of thermal stresses. Their accumulation resulted in the initiation of small cracks that gradually propagated and merged during further forging cycles.

Figure 11 presents the fracture surface of a crack observed in area 3 shown in Figure 1. The morphology of the fracture indicates a brittle transgranular failure mechanism propagating along cleavage planes. This type of cracking, characterized by crack growth through the grains, is typical of thermally and mechanically overloaded forging tools. Three distinct zones can be identified in the image. At the bottom lies the working surface of the tool, which was directly exposed to high thermal and mechanical loads due to contact with the heated billet. Just above this area is a narrow band (approximately 100 μm) of transcrystalline cracking. This cleavage-type fracture is inherently brittle, although it may have been initiated by localized plastic deformation. The uppermost zone of the fracture exhibits intergranular cracking, which propagates along grain boundaries. This form of failure is commonly associated with prolonged mechanical loading at elevated temperatures. Its presence indicates a progressive structural degradation initiated by thermal fatigue. The crack likely continued to propagate under operational stresses, potentially leading to the spalling of material from the tool surface.

Based on macroscopic observations, microstructural analysis using OM and SEM, hardness distribution across the tool cross-section, and 3D scanning analysis, the identification of the degradation mechanisms marked A–G in Figure 4 was performed. The individual mechanisms were assigned to specific regions based on characteristic morphological features: abrasive wear (A), evidenced by surface scratching in the spider-web region; thermal fatigue (B), manifested by a network of microcracks perpendicular to the working surface; initiation of fatigue cracks (C), indicated by visible microcracks; local chipping and partial melting (D), associated with topographical changes and adhesion traces; adhesive wear

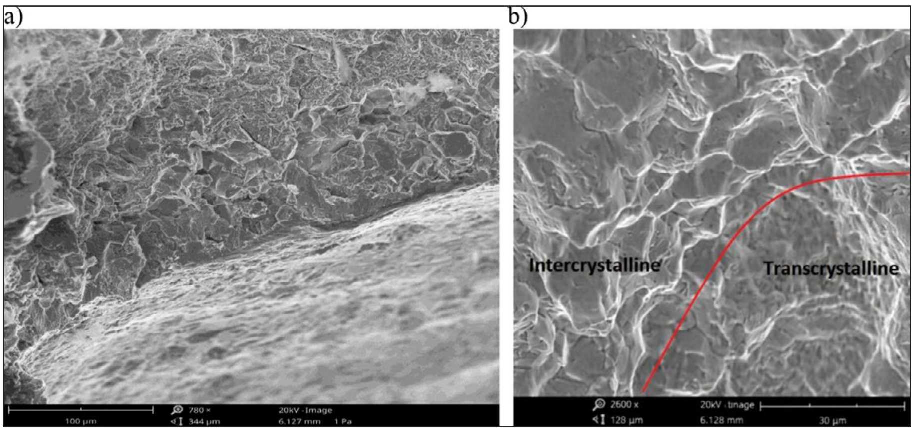


**Figure 11.** Fracture at the die crack location (a) and areas of transcrystalline and intercrystalline fracture (b) of the die in the area 3 shown in Figure 1

(E), evidenced by transferred workpiece material; abrasive-erosive wear (F), characterized by a surface appearance typical of pressurized material flow; and plastic deformation (G), confirmed by local dimensional changes identified through 3D scanning (Figure 12).

In summary, the conducted investigations emphasized significant limitations in the investigated tool durability, arising from both microstructural anomalies and suboptimal operational and thermal conditions. The observed degradation mechanisms, particularly thermomechanical fatigue and abrasive wear, underscore the need for thorough monitoring of the tool condition and optimization of heat treatment and operational parameters to enhance resistance as well as extend the service life of the tool. Moreover, the slightly elevated phosphorus content exceeding the normative limit specified by EN ISO 4957:2018 and shown in Table 1, may further impair the ductility of the material and promote brittleness, which is particularly unfavorable under dynamic and thermal loads during tool operation. The low content of chromium, molybdenum, and vanadium limits the potential benefits of these alloying elements on wear resistance, hardness, and fatigue strength, as confirmed by the observed surface damage and crack initiation.

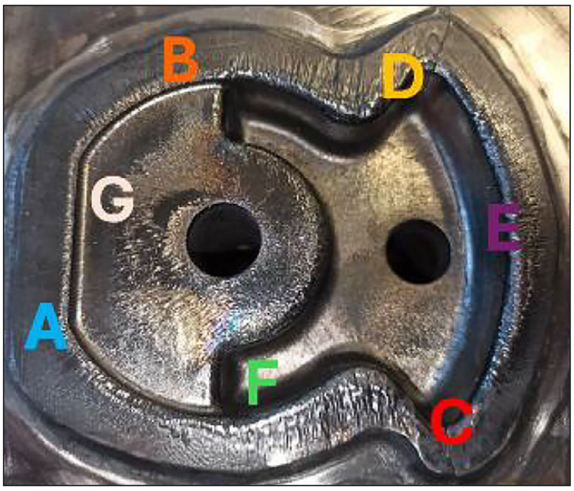


**Figure 12.** Identified wear and surface degradation mechanisms of the bottom die: A – abrasive wear, B – thermal fatigue, C – fatigue crack initiation site, D – local chipping and partial melting, E – adhesive wear, F – abrasion–erosion wear, G – plastic deformation

Numerical analysis revealed a highly non-uniform distribution of mechanical and thermal fields within the working area of the die insert. Figure 13 shows the equivalent stress distribution, Figure 14a shows the maximum principal stress $\sigma_1$, Figure 14b shows the mean stress, Figure 15b shows the elastic strain distribution, and Figure 15a shows the temperature distribution. A comparison of these results allowed identifying not only the areas of greatest tool loading but also the likely mechanism of crack initiation and propagation observed after service.

The equivalent stress distribution (Figure 13) indicates that its highest values occurred locally within the inner transition radii of the die and in the areas of abrupt changes in the direction of material flow. At the same time, most of the insert's volume was subjected to significantly lower stress levels, indicating that the critical condition did not affect the entire tool but was associated with local stress concentrations in the near-surface layer. A similar distribution of the elastic strain, which occurred in the same geometric zone, was also noticed. This indicates a local accumulation of elastic energy in the areas potentially susceptible to microcrack initiation.

The distribution of the maximum principal stress $\sigma_1$ (Figure 14a) showed, that in the zones of increased values of equivalent stress, local positive values of $\sigma_1$ were also observed, reaching

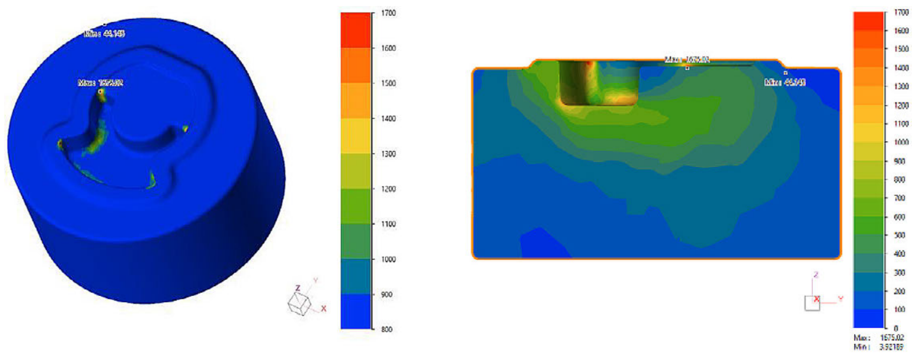

**Figure 13.** Equivalent stress distribution (MPa) in the investigated tools

a) b)

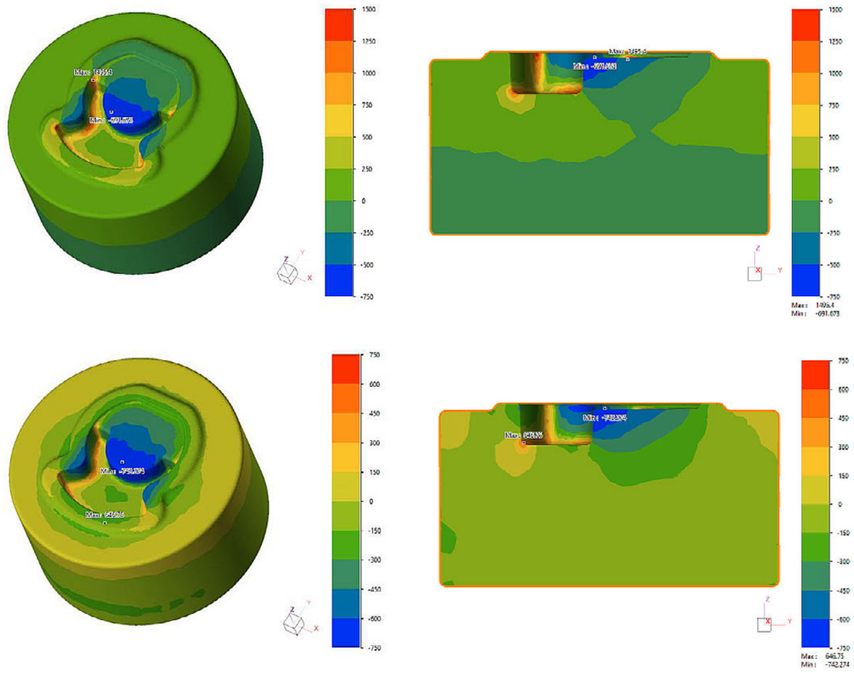

**Figure 14.** Maximum principal stress $\sigma_1$ (a) (MPa) and mean stress (MPa) distribution (b) in the investigated tools

approximately 1495 MPa. This indicates that in selected areas of the die's working surface, a stress state conducive to crack initiation was present. At the same time, the distribution of mean stress (Figure 14b) revealed the presence of local positive values, reaching approximately 647 MPa, in the vicinity of areas of maximum equivalent stress. The combination of high equivalent stress, positive principal stress, and positive mean stress indicates a particularly unfavorable loading condition from the perspective of the tool's fatigue life.

An additional factor contributing to the tools degradation process was the uneven temperature distribution (Figure 15a). The maximum tool

a) b)

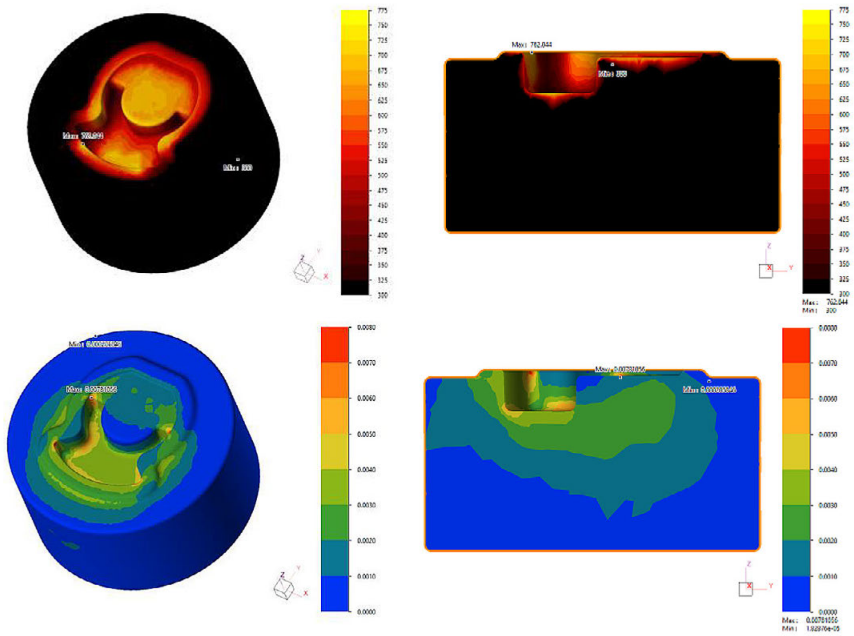

**Figure 15.** Distribution of temperature (°C) (a) and elastic strain (b) in the investigated tools

temperature reached approximately 762 °C and was concentrated in the areas where the forging material came into direct contact with the die's working surface. These zones partially overlapped with the areas of elevated stresses and elastic strain (Figure 15b), indicating the simultaneous interaction of the mechanical and thermal loads. Such conditions promote the development of thermal-mechanical fatigue, particularly in tool steel operating cyclically under hot forging conditions.

The most important result of the analysis is the agreement between the areas indicated by the FEM simulation and the actual crack path of the tool. The crack propagated along a line passing through the zone of the inner radius of the die cavity, then through the area of geometric narrowing, and further toward the upper part of the die insert. This path corresponds to the areas where local maxima of equivalent stress, positive values of principal stress $\sigma_1$, and increased elastic strain were observed in the simulation. It is particularly significant that the crack origin is located in a region where geometric narrowing, high stress concentration, and local tensile stresses occur simultaneously. This consistency indicates that the crack was not a random service-induced failure, but rather the result of a local accumulation of unfavorable mechanical and thermal conditions. In the initial stage, microcracks may have been initiated on the surface within the transition zone due to high stresses and cyclic temperature gradients. Subsequently, the presence of positive principal stresses facilitated the opening of the crack and its further propagation along a path consistent with the local stress concentration pattern. The results confirm that the dominant failure mechanism in the die insert was the thermomechanical fatigue initiated in the stress concentration zone.

## Mechanical properties

Hardness tests were conducted on two specimens (specimens taken from areas 2 and 3 shown in Figure 1) in cross-section and on the working surface of the tool. As illustrated in Table 2, the hardness distribution is comparable on the cross-section of the tool and the working surface of the die.

The hardness distribution presented in Table 2 indicates significant heterogeneity of the subsurface layer resulting from cyclic thermo-mechanical loading during the forging process. Local hardness increases exceeding 57 HRC may be associated with secondary hardening effects caused by repeated thermal exposure and precipitation of alloy carbides in the near-surface region of the die. Additionally, the previously identified microstructural banding may also contribute to local hardness variations due to the anisotropic character of the material microstructure. The surface hardness of the die insert depends on the exposure of the tool to cyclic heating and rapid cooling, which causes continuous hardening and strengthening of the working layer of the tool. At a distance of up to about 3 mm from the working surface of the tool, the hardness decreased as heat affects the subsurface layers of the material. However, these layers are not subjected to rapid cooling, which leads to partial tempering of the die material. At a distance of 3–4 mm from the working surface, the hardness increased again because these layers are relatively less affected by cyclic thermo-mechanical loading associated with the forging process. Therefore, the obtained values correspond to the hardness of the tool resulting from the initial heat treatment. The hardness distribution measured on the working surface indicates significant heterogeneity of hardness values. The accuracy of the measurements depends on the distance of the measurement point from the working edge. The working surface showed signs of wear, and additionally was not perfectly flat, causing in variations in hardness in the measurement distance from the working edge. Consequently, hardness measurements were not performed at identical distances from the working edge. The hardness test results indicated the presence of two characteristic zones within the tool. The first zone corresponded to the region of cyclic heating and cooling, which resulted in increased hardness, with measured values exceeding 57 HRC. The second zone was

**Table 2.** The hardness distribution on the cross-section of the tool and the working surface of the die. Measurements performed on sample taken from area 2 shown in Figure 1

| Distance [mm] | 1 | 2 | 3 | 4 | 5 | 6 | 7 | 8 | 9 | 10 |
|---|---|---|---|---|---|---|---|---|---|---|
| On the cross-section | 55.8 | 53.4 | 53.4 | 57.2 | 54.6 | 55.5 | 55.9 | 55.6 | 57.8 | 57.0 |
| On the working surface | 55.6 | 54.6 | 54.8 | 58.5 | 57.2 | 58.3 | 57.0 | 57.5 | 54.9 | 55.1 |

the heat-affected zone (HAZ), where the material underwent tempering, leading to reduced hardness values of approximately 55 HRC. The observed hardness heterogeneity may additionally promote localized stress concentration and facilitate thermomechanical fatigue crack initiation in the most thermally loaded regions of the die. These observations remain consistent with the degradation mechanisms identified during the microstructural examinations and fracture surface analyses.

Hardness tests were also conducted on the sample taken from area 3 shown in Figure 1, at three locations on a cross-section of the tool. Figure 16 illustrates the areas of the tool cross-section at which the hardness was tested (Figure 16a) and the obtained hardness values (Figure 16b). It is evident that site “a” is indicative of the flash, wherein there is an absence of protracted interaction between the charge and the tool. The area “b” is characterized by a pronounced interaction between the charge and the tool. Conversely, area “c” exhibits an interaction between the charge and the tool, although to a significantly lesser extent than observed at area “b”. The results obtained are indicative of three distinct zones of the influence exerted by the forging temperature on the investigated tool. In the area marked “a” in Figure 16, the application of heat and rapid cooling resulted in the strengthening of the tool. In the second area (“b”), the working surface of the insert die is released through the dissipation of heat from the area a). In the third area (“c”), the hardness values obtained following the thermal treatment of the tool are presented. The greatest effect of heat on the hardness of the tool was observed at the inclined position in the forge, resulting in significant variations in the tool’s hardness along its cross-section. It has been demonstrated that the hardness of the material increases in direct proportion to the tempering temperature. The temperature at which a drop in hardness becomes observable is approximately 500°C. This phenomenon is attributed to the secondary hardness effect, which leads to an increase in hardness during the process of steel tempering. This is due to the transformation of residual austenite and release of new alloy carbides. It is reasonable to hypothesize that the tempering temperature of the die was approximately 500°C, based on the hardness values obtained during the hardness tests. The maximum hardness values measured in the tool were of approximately 56÷58 HRC. In accordance with the established standard, the hardness of a forging tool produced from 1.2343 steel should be approximately 52 HRC. This may indicate that the heat treatment parameters or operational thermal exposure influenced the final hardness state of the tool. The hardness distribution across the tool cross-section showed significant heterogeneity, caused by localized heating and cooling cycles during forging operations. The highest hardness values exceeding 57 HRC in the working layer of the tool indicate a secondary hardening effect related to structural transformations occurring during tempering at approximately 500°C. Concurrently, the hardness reduction in the heat-affected zone proves partial tempering of the material, which is corroborated by impact toughness test results consistent with the temperature range of 500–550°C. It should be noted, however, that the hardness values exceed normative recommendations, which may indicate

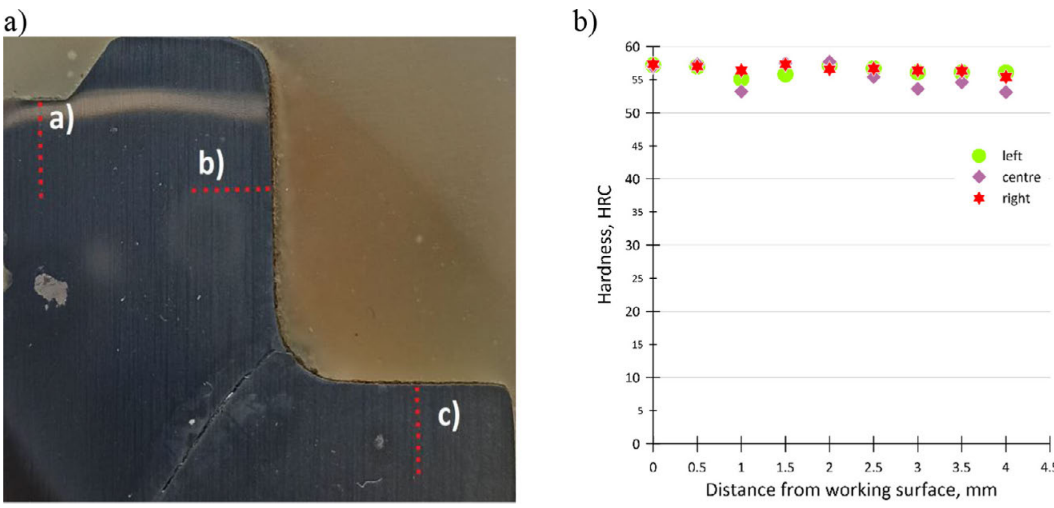


**Figure 16.** Hardness measurements (a) and hardness distribution (b) on sample taken from area 3 shown in Figure 1 at three locations on a cross-section of the tool

an improper heat treatment process, potentially adversely affecting tool durability and crack resistance. Six impact test specimens were fabricated from the specimens taken from the investigated die from the areas 5 and 6 shown in Figure 1. Impact strength was tested on a Charpy hammer. The test specimens were characterized by a standardized geometry, with a "V" notch cut on selected surface of the sample. The impact strength of the investigated steel was approximately 26 J/cm$^2$, however, the average impact strength measured on the samples taken from the area 5 was 23.9 J/cm$^2$, and the average impact strength measured on the samples taken from the area 6 was 27.5 J/cm$^2$, which indicates some anisotropy of the mechanical properties of the investigated steel resulting from microstructural banding resulting from the rolling process.

A comparison of the obtained impact strength values with literature data for 1.2343 steel [46] indicates consistency with values reported for tempering temperatures in the range of approximately 500–550 °C. It is well known that increasing tempering temperature may improve impact toughness and ductility of the steel, although usually at the expense of reduced hardness.

The assessment of thermo-mechanical degradation mechanisms was based on microstructural observations, hardness distribution analysis, fracture morphology, industrial operating conditions, and characteristic degradation features widely reported in the literature for hot forging tools operating under industrial conditions.

## CONCLUSIONS

Microstructural analysis and mechanical property testing of the tool revealed that the investigated tool steel used for the die insert exhibits a microstructure typical of the steels subjected to quenching and tempering.

The presence of microstructural banding resulting from the rolling process may indicate local anisotropy of the material microstructure, which can potentially affect fatigue resistance and crack initiation, especially under cyclic thermomechanical loading conditions. This was confirmed by the anisotropy of the impact strength of the investigated steel measured on the samples taken from two areas 5 and 6 shown in Figure 1.

Microstructural examinations of the subsurface area demonstrated changes caused by the intense thermal influence from the heated billet, leading to partial strengthening and structural transformations, as well as revealing microstructural defects such as non-metallic inclusions and uneven structural recovery after plastic deformation. Observed thermal cracks and their propagation aligned with the banding direction of the microstructure confirm a damage mechanism based on thermomechanical fatigue, which is characteristic of the tools operating under cyclic temperature and stress variations.

Hardness measurements revealed a non-uniform distribution across the tool cross-section. The working layer exhibited values of 56–58 HRC, exceeding the recommended 52 HRC for 1.2343 steel, indicative of a secondary hardening effect and inadequate tempering conditions. The heat-affected zone showed reduced hardness of approximately 55 HRC consistent with partial tempering at approximately 500°C. The impact toughness (approx. 26 J/cm$^2$) corroborates a tempering temperature in the 500–550°C range.

The FEM analysis confirmed, that the dominant failure mechanism in the die insert was thermomechanical fatigue initiated in the stress concentration zone. The highest values of equivalent stress and maximum principal stress $\sigma_1$ occurred at the actual crack initiation area of the tool. The distribution of mean stress and temperature confirmed the presence of unfavorable conditions conducive to the development of thermal-mechanical fatigue. The actual fracture path showed a high degree of agreement with the critical zones predicted in the numerical analysis.

### Acknowledgements

Financial support of the Ministry of Science and Higher Education within the framework of the IMPLEMENTATION DOCTORATE 7th edition program (number of project: 68.10.110.01150.DWD/7/0283/2023) is greatly acknowledged. The authors also acknowledge the AGH University of Krakow for the support of this research within the Project IDUB (Excellence Initiative—Research University).

## REFERENCES

1. Emamverdian A.A., Sun Y., Cao C., Pruncu C., Wang, Y. Current failure mechanisms and treatment methods of hot forging tools (dies) – a review., Eng. Fail Anal. 2021; 129: 105678. https://doi.org/10.1016/j.engfailanal.2021.105678

2. Ficak G., Łukaszek-Sołek A., Hawryluk M. Durability of forging tools used in the hot closed die forging process—A review. Materials. 2024; 17(22):5407. https://doi.org/10.3390/ma17225407.
3. Abd Al-Kareem Ahmed I., Mohammed A.I., Allow M.A. Improvement of forging die life by failure mechanism analysis. J. Mech. Behav. Mater. 2021; 30(1): 309–317. https://doi.org/10.1515/jmbm-2021-0034
4. Chander S., Chawla V. Characterization and industrial performance evaluation of duplex-treated AISI H21 die steel during hot forging process. Matls. Perf. Charact. 2019; 8(1): 197–210. https://doi.org/10.1520/MPC20180152
5. Hawryluk M., Lachowicz M., Łukaszek-Sołek A., Lisiecki Ł., Ficak G., Cygan P. Structural features of fatigue crack propagation of a forging die made of chromium–molybdenum–vanadium tool steel on its durability. Materials. 2023; 16(12): 4223. https://doi.org/10.3390/ma16124223
6. Krawczyk J., Łukaszek-Sołek A., Lisiecki Ł., Śleboda T., Hawryluk M. Wear mechanisms of the forging tool used in pre-forming in a double forging system of truck parts. Materials. 2023; 16(1): 351. https://doi.org/10.3390/ma16010351
7. Krawczyk J., Łukaszek-Sołek A., Śleboda T., Lisiecki Ł., Bembenek M., Cieślik J., Góral T., Pawlik J. Tool Wear Issues in Hot Forging of Steel. Materials. 2023; 16(2): 471. https://doi.org/10.3390/ma16020471
8. Bouguecha A., Behrens B.-A., Bonk C., Rosenbusch D., Kazhai, M. Numerical die life estimation of a crack susceptible industrial hot forging process. Proceedings of the 20th International Esaform Conference On Material Forming: Esaform 2017. AIP Conf. Proc. 2017; 1896(1): 190012. https://doi.org/10.1063/1.5008225
9. Wang W., Wang W., Changwen H., Song J., Baoguo X., Zhang, Z. Cracking failure analysis of steel piston forging die. Eng. Fail. Anal. 2022; 138: 106291. https://doi.org/10.1016/j.engfailanal.2022.106291
10. Pandya V.A., George P.M. Analysis of die stress and forging force for DIN 1.2714 die material during closed die forging of anchor shackle. Mater. Today: Proc. 2021; 45(6): 4695–4701. https://doi.org/10.1016/j.matpr.2021.01.121
11. Kang J.H., Park I.W., Jae J.S., Kang S.S. A study on die wear model of warm and hot forgings. Metals and Materials. 1998; 4: 477–483. https://doi.org/10.1007/BF03187813
12. Behrens B.A., Yilkiran T. Influence of the fabrication method on the wear resistance of hot forging dies. Prod. Eng. Res. Devel. 2012; 6: 267–276. https://doi.org/10.1007/s11740-012-0373-y
13. Dalbosco M., da Silva Lopes G., Schmitt P.D., Pinotti L., Boing D. Improving fatigue life of cold forging dies by finite element analysis: A case study. J. Manuf. Process. 2021; 64: 349–355. https://doi.org/10.1016/j.jmapro.2021.01.039
14. Killmann M., Merklein M. Fatigue testing of cold forging tools using elastomer compression. CIRP Annals. 2023; 72(1): 241–244. https://doi.org/10.1016/j.cirp.2023.03.007
15. Pereira M.P., Weiss M., Rolfe B.F., Hilditch T.B. The effect of the die radius profile accuracy on wear in sheet metal stamping. Int. J. Mach. Tools Manuf. 2013; 66: 44–53. https://doi.org/10.1016/j.ijmachtools.2012.11.001
16. Lee, R.S., Jou, J.L. Application of numerical simulation for wear analysis of warm forging die. J. Mater. Process. Technol. 2003; 140(1–3): 43–48. https://doi.org/10.1016/S0924-0136(03)00723-4
17. Veiga-Piñeiro G., Martin-Ortega E., Pérez-Betanzos S. Thermal management in multi-stage hot forging: computational advances in contact and spray-cooling modelling. Materials. 2025; 18(14): 3318. https://doi.org/10.3390/ma18143318
18. Hawryluk M., Gronostajski Z., Ziemba J., Dworzak Ł., Jabłoński P., Rychlik M. Analysis of the influence of lubrication conditions on tool wear used in hot die forging processes. Eksploatacja i Niezawodność – Maintenance and Reliability. 2018; 20(2): 169–176. https://doi.org/10.17531/ein.2018.2.01
19. Fleming, C., Kerr, W., Krishnamurthy, B., et al. Quasi-industrial accelerated testing of a HIPIMS deposited nano-layered CrAlYN/CrN coating for improving hot forging die life of nitrided H13 steel. J. Manufac. Process. 2025; 143: 132–150. https://doi.org/10.1016/j.jmapro.2025.03.106
20. Li X., Ma J., Wang Y., Jiang Y. A Novel Nano-Structured Die Steel with High Strength and High Thermal Stability. Acta Metall. Sin. (Eng. Lett.). 2025; 38: 1594–1603. https://doi.org/10.1007/s40195-025-01881-7
21. Yuan Y., Lin Y., Wang W., Zhang B., Shi R., Zhang Y., Xie J., Wu C., Mao F. Study on high-temperature constitutive model and plasticity of the novel Cr-Mo-V hot-work die steel forging. Materials. 2024; 17(24): 6071. https://doi.org/10.3390/ma17246071
22. Hawryluk M., Dudkiewicz Ł., Borowski J., Marzec J., Tkocz R. Increasing the working time of forging tools used in the industrial process of producing a disk-type forging assigned for a gearbox through the application of hybrid layers. Materials. 2024; 17(12): 3005. https://doi.org/10.3390/ma17123005
23. Chantziara K., Nikas D., Bergstróm J., Grehk M., Pappa M., Michailidis N. High and very high cycle fatigue behavior of an additive manufactured hot-work tool steel. Mater. Sci. Eng. A. 2024; 917: 147401. https://doi.org/10.1016/j.msea.2024.147401
24. Li X., Ma J., Wang Y., Jiang Y. A novel nano-structured die steel with high strength and high thermal stability. Acta Metall. Sin. (Eng. Lett.), 2025; 38: 1591–1603. https://doi.org/10.1007/s40195-025-01881-7

25. Duchek M., Šuchmann P., Režnar J., Krejčík J., Marek R. Development of modified versions of 1.2343 tool steel. Conference Proceedings, 21st International Conference on Metallurgy and Materials METAL, 2012, 374–377. http://www.scopus.com/inward/record.url?eid=2-s2.0-84923902692&partnerID=MN8TOARS
26. Yuan Y., Lin Y., Wang W., (...), Mao F. Study on high-temperature constitutive model and plasticity of the novel Cr-Mo-V hot-work die steel forging. Materials. 2024; 17(24): 6071. https://doi.org/10.3390/ma17246071
27. Şengül Ü., Sengül A.B. Hot forging die material selection using fuzzy multi-criteria decision making methods. Mater. Today Commun. 2024; 38: 108352. https://doi.org/10.1016/j.mtcomm.2024.108352
28. Jeong D.J, Kim D.J, Kim J.H, Kim B.M., Dean T.A. Effects of surface treatments and lubricants for warm forging die life. J. Mater. Process. Technol. 2001; 113(1–3): 544–550. https://doi.org/10.1016/S0924-0136(01)00693-8
29. Lee, H.C., Kim, B.M., Kim, K.H. Estimation of die service life in hot forging, considering lubricants and surface treatments. Proceedings of the Institution of Mechanical Engineers, Part B: J. Eng. Manuf. 2003; 217(7): 1011-1022. https://doi.org/10.1243/09544050360686860.
30. Behrens B.-A., Lachmayer R., Malik, I., Bonhage P., Sauthoff B., Gottwald, P. Sensor technology for hot forging tools - Temperature control of hot forging dies increases precision and reduces wear. WT Werkstattstechnik. 2015; 105(10): 692–696. https://doi.org/10.37544/1436-4980-2015-10-28
31. Schmid S.R., Liu J., Sellés M.A., Pasang T. Advanced interface models for metal forming simulations. Comput. Mater. Scie. 2013; 79: 763–771. https://doi.org/10.1016/j.commatsci.2013.07.025
32. Veiga-Piñeiro G., Martin-Ortega E., Pérez-Betanzos S. Thermal management in multi-stage hot forging: Computational advances in contact and spray-cooling modelling. Materials. 2025; 18(14): 3318. https://doi.org/10.3390/ma18143318
33. Razali M.K., Wan K.S., Irani M., Kim M. Ch., Joun M.S. Practical quantification of the effects of flow stress, friction, microstructural properties, and the tribological environment on macro- and micro-structure formation during hot forging. Tribol. Int. 2021; 164: 107226. https://doi.org/10.1016/j.triboint.2021.107226
34. Rajiev, R., Sadagopan, P. Simulation and Analysis of hot forging dies for Pan Head bolt and insert component. Mater. Today: Proc. 2018; 5(2–2): 7320–7328. https://doi.org/10.1016/j.matpr.2017.11.401
35. Kang J.H., Park I.W., Jae J.S., Kang S.S. A study on die wear model of warm and hot forgings. Metals and Materials. 1998; 4: 477–483. https://doi.org/10.1007/BF03187813
36. Behrens B.A., Rosenbusch D., Wester H., Siring J. Numerical investigations on stresses and temperature development of tool dies during hot forging. Key Eng. Mater. 2022; 926: 559–568. https://doi.org/10.4028/p-sf68jl
37. Joshy S., Kumar T.M.A., Asok N.N., Suraj R., Joseph K.P. Optimisation of Parameters in Numerical Simulation of Hot Forging Using Taguchi Approach. In: Vučinić, D., Chandran, V., Mahbub, A.M., Sobhan, C.B. (eds). Applications of Computation in Mechanical Engineering. Lecture Notes in Mechanical Engineering. 2023: 215–225. https://doi.org/10.1007/978-981-19-6032-1_17
38. Bendjoudi Y., Becker E., Bigot R., Amirat A. Contribution in the evaluation of a performance index of hot forging dies. Int. J. Adv. Manuf. Technol. 2017; 88: 1187–1201. https://doi.org/10.1007/s00170-016-8829-4
39. Behrens B.A., Hadifi T. XII International Conference on Computational Plasticity: fundamentals and applications (COMPLAS 2013). 2013: 1119–1129. https://hdl.handle.net/2117/183244
40. Dudkiewicz Ł., Hawryluk M. Low-waste technology for high-precision connecting rod forging manufacturing. Materials, 2025; 18(2): 443. https://doi.org/10.3390/ma18020443
41. Kim D.H., Lee H.C., Kim B.M., Kim K.H. Estimation of die service life against plastic deformation and wear during hot forging processes. J. Mater. Proc. Tech. 2005; 166(3): 372–380. https://doi.org/10.1016/j.jmatprotec.2004.07.103
42. Virtanen E., van Tyne C.J., Levy B.S., Brada G. The tempering parameter for evaluating softening of hot and warm forging die steels. J. Mater. Proc. Tech. 2013; 213(8): 1364–1369. https://doi.org/10.1016/j.jmatprotec.2013.03.003
43. Schlayer M., Warwas M., Seifert T. A temperature-dependent viscoplasticity model for the hot work steel X38CrMoV5-3, including thermal and cyclic softening under thermomechanical fatigue loading. Materials. 2023; 16(3): 994. https://doi.org/10.3390/ma16030994
44. Alessio A., Antonelli D., Doglione R., Genta G. Die wear reduction by multifactorial Design of Experiments applied to forging simulations. Procedia CIRP. 2022; 112: 424–429. https://doi.org/10.1016/j.procir.2022.09.031
45. Behrens B.-A., Lippold L. Influence of shot peened surfaces on friction in hot forging. Surf. Topogr.: Metrol. Prop. 2018; 6: 045005. https://doi.org/10.1088/2051-672X/aae91c
46. SIJ Metal Ravne, d.o.o. SITHERM S350R specification sheet. https://steelselector.sij.si/steels/ravnex-dc.html